Author Manuscript

Author Manuscript

Author Manuscript

Author Manuscript

HHS Public Access

Author manuscript

Brain Res. Author manuscript; available in PMC 2021 July 01.

Published in final edited form as:

Brain Res. 2015 September 04; 1619: 72–83. doi:10.1016/j.brainres.2015.01.055.

Coiled polymeric growth factor gradients for multi-luminal neural chemotaxis

Nesreen Zoghoul Alsmadi[a], **Lokesh S. Patil**[b], **Elijah M. Hor**[b], **Parisa Lofti**[b], **Joselito M. Razal**[c], **Cheng-Jen Chuong**[b], **Gordon G. Wallace**[c], **Mario I. Romero-Ortega**[a,*]

[a]Department of Bioengineering, University of Texas at Dallas, 800 W. Campbell Rd., EC39, Richardson, 75080 TX, USA

[b]Department of Bioengineering, University of Texas Arlington, Arlington, TX, USA

[c]ARC Centre of Excellence for Electromaterials Science, Intelligent Polymer Research Institute, AIIM Facility, Innovation Campus, University of Wollongong, Wollongong, NSW 2522, Australia

Abstract

In the injured adult nervous system, re-establishment of growth-promoting molecular gradients is known to entice and guide nerve repair. However, incorporation of three-dimensional chemotactic gradients in nerve repair scaffolds, particularly in those with multi-luminal architectures, remains extremely challenging. We developed a method that establishes highly tunable three-dimensional molecular gradients in multi-luminal nerve guides by anchoring growth-factor releasing coiled polymeric fibers onto the walls of collagen-filled hydrogel microchannels. Differential pitch in the coiling of neurotrophin-eluting fibers generated sustained chemotactic gradients that appropriately induced the differentiation of Pheochromocytoma (PC12) cells into neural-like cells along an increasing concentration of nerve growth factor (NGF). Computer modeling estimated the stability of the molecular gradient within the luminal collagen, which we confirmed by observing the significant effects of neurotrophin gradients on axonal growth from dorsal root ganglia (DRG). Neurons growing in microchannels exposed to a NGF gradient showed a 60% increase in axonal length compared to those treated with a linear growth factor concentration. In addition, a two-fold increment in the linearity of axonal growth within the microchannels was observed and confirmed by a significant reduction in the turning angle ratios of individual axons. These data demonstrate the ability of growth factor-loaded polymeric coiled fibers to establish three-dimensional chemotactic gradients to promote and direct nerve regeneration in the nervous system and provides a unique platform for molecularly guided tissue repair.

Keywords

Axon guidance; Nerve growth factor; Dorsal root ganglia; Sensory neurons; Nerve scaffolds

[*]*Corresponding author*. Fax: +1 972 883 4653. Mario.romero-ortega@utdallas.edu (M.I. Romero-Ortega).

Author Manuscript Author Manuscript Author Manuscript Author Manuscript

1. Introduction

In the developing peripheral nervous system neural cells elongate their axons towards proper target cells instructed by gradients of guidance molecules, which may be bound to the cell membranes or extracellular matrix (ECM), or diffused from their release sites into the extracellular fluid. The growth cone at the leading edge of growing axons bears receptors that bind to guidance cues, thereby sensing both the chemical composition and steepness of the molecular gradient. This chemotactic molecular recognition inform the growing neurons about the permissive or repellent nature of the environment, guiding their growth along attractive molecular gradients (Kolodkin and Tessier-Lavigne, 2011; Arimura and Kaibuchi, 2007; Song and Poo, 2001; Gallo and Letourneau, 1999; Dickson, 2002). In addition to translate the chemotactic information from it's environment, the growth cone also senses its molecular composition (i.e., collagen, fibronectin, and laminin) and the physical characteristics of the ECM, such as matrix pore size and stiffness (Flanagan, 2006; Dodla and Bellamkonda, 2008; Adams et al., 2005; Wu et al., 2012).

In the adult peripheral nervous system, injured sensory axons from the central branch of the dorsal root ganglia (DRG) regenerate spontaneously, but are unable to enter the hostile environment of the adult spinal cord unless enticed by the induced expression of NGF or fibroblast growth factor (FGF) (Romero et al., 2001). Similarly, sensory and motor axons in adult peripheral nerves regrow spontaneously after injury, but often fail to accurately reinnervate their original skin and muscle targets, due in part to the absence of proper molecular cues. Indeed, re-establishment of neurotrophic factor (NTF) chemotactic gradients has been shown to steer axonal growth and target innervation (Tang et al., 2007; Ziemba et al., 2008; Hu et al., 2010). These reports provide strong support for the use of NTF gradients in peripheral nerve injury repair (Zochodne, 2012). However, incorporation of NTF gradients into tissue engineered nerve scaffolds is extremely challenging due to the lack of NTF delivery methods that provide sustained three-dimensional molecular gradients and ECM support for optimal axonal elongation and directed growth.

A number of reported technologies can either establish molecular gradients through immobilization on photo-labile hydrogels, which does not provide sustained release (Kapur and Shoichet, 2004), or by infusion of differential concentrations of growth factors to the walls of nerve conduits, but lack ECM support (Tang et al., 2013). An ideal method will provide both luminal ECM and spatio-temporal controlled three-dimensional molecular NTF gradients within physiological range (Tonra et al., 1998).

Multi-luminal nerve scaffolds with ECM fillers are of particular interest as they provide increased surface area for nerve regeneration compared to simple nerve guides. We recently reported that multi-luminal nerve scaffolds fabricated with hydrogel microchannels and collagen fillers successfully bridged a nerve injury gap, by linearly restricting axonal regeneration and enticing the regeneration of fascicular-like tissue (Tansey et al., 2011). We have also shown that adding PLGA microparticle release of vascular endothelial growth factor (VEGF) into the collagen-filled microchannels, increases angiogenesis from aorta explants (Dawood et al., 2011). However, loading the polymeric microparticles into the microchannels to provide sustained growth factor support is not optimal, as they are

Author Manuscript Author Manuscript Author Manuscript Author Manuscript

suspended in the luminal space and partially block nerve growth. Furthermore, this approach does not allow for the establishment of needed molecular gradients. In this study, we report a novel strategy for the establishment of three-dimensional NTF gradients by deployment of coiled polymeric biodegradable fibers onto the wall of hydrogel microchannels filled with collagen. A mathematical model was used to predict the NTF diffusion from the polymeric coils into the complex hydrogel/collagen matrix and was validated by *in vitro* DRG neural growth assays, which provided evidence of chemotactic nerve regeneration along the three-dimensional NGF gradients. This work provides a unique platform for an improved biomimetic design of multi-luminal engineered nerve scaffolds aimed at improving functional recovery after nerve repair.

2. Materials and methods

2.1. Intraluminal NTF-collagen gradient

Current nerve repair technologies use either empty nerve guides supplemented with uniform growth factor release or gradient NTF release from the walls of the nerve guide, which lacks ECM luminal fillers or multi-luminal structures (Fig. 1A–a) (Tang et al., 2013). Here, we report a novel method that achieves sustained growth factor gradient release through the production of molecular gradients in collagen-filled multi-luminal nerve guides (Fig. 1A–b). This protocol was first demonstrated by coiling NGF-eluting polymeric biodegradable fibers over titanium rods, which were inserted into a transparent multi-luminal matrix (TMM) casting device as reported previously (Fig. 1B) (Dawood et al., 2011). Briefly, the TMM consists of a plastic frame with openings at opposite ends, through which the titanium rods are inserted (Fig. 1B–i). Once in place, 1.5% (by weight) agarose is gelled over the metal rods, the coil exposed to the agarose (i.e., not in contact to the metal rod) is effectively embedded, and remains attached to the hydrogel after gelation. Collagen IV is then added to the “loading” well of the TMM. Subsequent removal of the metal rod leaves the polymeric fiber anchored to the agarose and the portion that faced the metal rod, exposed to the lumen of the channel. Simultaneously, the negative pressure created by the metal rod removal from the agarose, draws the collagen from the loading well into the microchannels completely filling the luminal space (Fig. 1B–ii and iii). The result is of microchannels casted in agarose with polymeric coils anchored to the walls from where they release their protein load overtime into the collagen filler, effectively providing a source of sustained three-dimensional gradient release. Densitometry of the fiber-containing a flourescent label (Cy3 IgG; red) shows the formation of the gradient (Fig. 1C–c). Quantification of the protein release was done by cutting the TMM gel in half and measuring the BSA release over a 24 h window from the low (TMM-L) and high (TMM-H) ends of the gel. The result was an approximately 40-fold increase in protein release from the TMM-H coils (Fig. 1D). Confocal imaging of the TMM showed coiled PLGA fibers loaded with Cy3-IgG affixed to the walls of an agarose microchannel filled with collagen-Cy2-IgG (green) filler. The coils were fabricated in a single batch to ensure reproducibility in NTF release.

2.2. Growth factor-releasing coiled polymeric fibers

Two different polymer types were used to fabricate the coiled fibers: poly-lactic-co-glycolic acid (PLGA 85:15; 135 kDa) 30 μm, and ELUTE® Biodegradable Polydioxanone (PDO) 50

Author Manuscript Author Manuscript Author Manuscript Author Manuscript

μm. The release properties from PLGA and PDO has been reported previously (Zilberman, 2005). PLGA fibers were fabricated by wet-spinning as reported elsewhere (Nelson et al., 2003). Briefly, a 20% PLGA solution was prepared in dichloromethane (DCM; Sigma-Aldrich, St. Louis, MO) and 2 μl (1 μg/μL) of NGF was added to the PLGA solution and sonicated for 1 min. The solution was then dispensed into a circulating isopropanol coagulation bath using a syringe pump (1.8 ml/h). The resulting fiber was collected onto a rotating spool (8.5 m/min). For PC12 cells experiments, dried PLGA coil fibers (no protein) were incubated with NGF (10 μg/ml; Invitrogen, Carlsbad, CA), BSA (20 mg/ml; Sigma-Aldrich, St. Louis, MO) or cyanine dye-3 (cy3; 5 μg/ml; Jackson ImmunoResearch Lab, Inc., West Grove, PA) overnight.

The PDO fibers were fabricated under a proprietary process by TissueGen Inc. with encapsulated NGF-containing microparticles. The PDO fibers were coiled 80 times over titanium metal rods (0.25 mm diameter × 17 mm length; SmallParts, Logansport, IN) either equally (uniformly; U) or differentially spaced (gradient; G) at 15, 25, and 40 turns over 3.33 mm longitudinal area and covering a 10–100 ng/ml concentration range (TissueGen Inc, Dallas, TX). Both types of fibers were used in PC12 culture studies. Only the PDO fibers were used for the DRG experiment as TissueGen Inc. developed a process for precise control of the coil pitch. Quantification of NGF by ELISA showed that PLGA and PDO fibers released 4.40 and 5.36 pg/cm over 7 days, respectively. In the microchannels, the volume is restricted to 0.49 μl, therefore a total of 8.88 and 11.43 ng/ml of NGF were released by PLGA and PDO fibers over 1 week, respectively. The coiled fibers on the metal rods were dried at room temperature and stored at −20 °C until used.

2.3. PC12 cell culture

PC12 cells at a 1×10^6 cell/ml plating density were cultured in regular 2D culture plates and exposed to a 10–100 ng/ml NGF range to determine their neurite differentiation response as indicated by the neuron-like differentiation and neurite extension. As expected, PC12 cells showed neurite elongation proportionally to the NGF concentration (Fig. 2A–C). ELISA quantification showed that the PDO fibers release more NGF compared to the PLGA fibers during the 7-day testing (Fig. 2D), but both fibers were comparable in inducing differentiation of PC12 cells (Fig. 2E). We then compared BSA- or NGF-eluting PLGA fibers after deploying them in the TMM casting device as described above. Under sterile conditions, the casting device was placed over a glass slide in a cell culture dish and 1.5% ultrapure agarose was used to cover the fibers. After gelation, PC12 cells (1×10^6 cell/ml) suspended in a telomeric chicken collagen (85% type I, 15% type II; Millipore) were loaded onto the casted 250 μm OD hydrogel microchannels by the negative pressure generated. The TMM cell cultures were incubated for 72 h in RPMI-1640 medium (Hyclone SH30027.02) supplemented with 10% HS, 5% FBS, and 1% pen/strep and maintained at 37 °C and 5% CO_2. At the end of the study, the cell cultures were fixed in 4% paraformaldehyde (PFA), extensively rinsed with 1 × PBS, and stained with green phalloidin (Fig. 2F–H). The cells were then imaged at both ends of the gradient coils and the neurite length quantified at the low (TMM-L) and high (TMM-H) coil number ends of the microchannels. The neurite length estimated from these studies was compared to that obtained with the calibrated 2D

Author Manuscript Author Manuscript Author Manuscript Author Manuscript

PC12 differentiation assay, and used to estimate the luminal NGF concentration in the microchannels (Fig. 2I–J).

2.4. NGF release quantification

Fifteen centimeters of PLGA fiber and 10 cm of PDO fibers (n=3) were incubated in PBS (1.5 ml). At specific time points, including 0, 1, 2, 6, 24, and 168 h at 37 °C, supernatant was collected and replaced with fresh buffer. The drug release kinetic was determined using enzyme linked immunosorbent assays (ELISA) kit according to manufacturer's instructions (Invitrogen, Carlsbad, CA).

2.5. BSA coil release profile in hydrogel

Three centimeters of PLGA fiber were deployed in the TMM casting device in a gradient configuration (n=3). The agarose gels were cut into two different segments with low (L) or high (H) number of coils. To characterize the release, each segment was separately incubated in 1 ml of 1 × PBS at 37 °C for 24 h. At specific time points, including 0, 1, 2, 4, 8, 12, and 24 h, supernatant was collected and replaced with fresh buffer. A BCA protein assay kit (Thermoscientific Pierce) was used to determine protein content in each segment.

2.6. Modeling the diffusion release of growth factors

We modeled the diffusion release of growth factors from polymeric coils in both uniform and gradient configurations positioned in collagen-filled microchannels, surrounded by agarose, with the finite element method using COMSOL 4.2 (COMSOL, Inc.). The protein release profile from a polymeric coil was modeled by fitting the release data from 0 to 10 days provided by the manufacturer to a power law equation, expressed as (Ramanujan et al., 2002)

$$f = Kt^n$$

where f is the fractional drug release, and t is the time in hours. Values for K and n were found to be 0.55 and 0.11 respectively. A combination of Brinkman and Carman-Kozeny models was used to estimate molecular diffusivity of the drug used in water, in 1.5 wt% agarose, and in 0.3 wt% collagen (Ramanujan et al., 2002). Values of drug molecular diffusivity in collagen, agarose and geometric dimensions used for the design of the device and the modeling are summarized in Table 1. Diffusion of the drug molecules is governed by Fick's 2nd law, written as (Murray, 1989)

$$\frac{\partial C}{\partial t} = \nabla . (D \nabla C) + R$$

where C is the concentration in mol/m^3, D denotes the diffusivity, t the time in seconds, and R represents the rate of drug release from the PLGA coil in mol/m^{3}s. Using 2nd order Lagrangian tetrahedral volume element, we discretized the computational domain with a total of 2.1 and 2.3 million elements for U and G model, respectively. The Newmark integration scheme was used to solve the transient diffusion equation.

Author Manuscript Author Manuscript Author Manuscript Author Manuscript

2.7. DRG explant growth in TMM microchannels

Neonatal (P0–P4) DRGs were isolated from normal mice and placed at one end of the TMM microchannels containing either U or G NGF-coils. The DRG cultures were cultured in Neurobasal A media (Sigma Aldrich) and maintained at 37 °C and 5% CO_2 for 7 days, fixed in 4% PFA, extensively rinsed in 1 × PBS and stained.

2.8. Immunostaining

TMM gels with PC12 cells were incubated in Oregon Green Phalloidin to label cytoskeletal elements. For DRG axonal growth, the tissue was incubated in 4% Donkey serum for 1 h, followed by incubation with a mouse anti-β tubulin III antibody (1:400; Sigma Aldrich) overnight at 4 °C. The gels were then incubated with Cy2-conjugated donkey anti-mouse IgG (1:400; Sigma Aldrich) and rinsed. Long-distance water immersion objectives on a Zeiss confocal microscope (Zeiss Axioplan 2 LSM 510 META) were used to evaluate the cellular staining and axonal growth directly within the hydrogel microchannels.

2.9. Image analysis and quantification

Neurite length in differentiated PC12 cells was evaluated inside the microchannels at low concentrated (TMM-L) and high concentrated (TMM-H) areas corresponding to different numbers of NGF-coils. Neurite length was measured from the cell body to the distal end of the neurites. Only cells with neurites longer than the cell diameter were considered for quantification, using Axiovision LE software (CarlZeiss, Axiocam, version 4.7.2), Zeiss LSM Image Browser (version 4.2.0.1). The axonal length of the DRG was quantified at 20× magnification from a z-stack (20 images each at 15.4 μm slice thickness). Axonal length was measured from the edge of the DRG to the growth cone terminal using Axiovision LE software and Zeiss LSM Image Browser (version 4.2.0.1). Segments were evaluated in areas with medium (1–8) or high (9–15) number of coils. Axonal turning angles were measured using Image J. Quantification of the turning angle was calculated as a ratio of the number of axons that turned to all the axons present. All experiments were performed in 3–6 replicates.

2.10. Statistical analysis

All data values were expressed as mean±standard error of the mean. The PC12 and DRG data were evaluated by ANOVA followed by Newman–Keuls Multiple Comparison using the Prism 4 software (GraphPad Software Inc.). Values with $p \leq 0.05$ were considered to be statistically significant.

3. Results

3.1. PC12 differentiation in a 3D NGF microgradient

To determine if the polymeric coils can be used to establish biologically active gradients of neural growth factors, we tested the ability of PC12 cells to differentiate in the lumen of the TMM microchannels onto which BSA or NGF-eluting coils were anchored to the hydrogel walls. Three days after seeding, only rounded undifferentiated cells were oberved in the controls (Fig. 2F). In contrast, those cultured with NGF-coils showed several degrees of neural differentiation as indicated by neurite elongation from the PC12 cell bodies (Fig. 2G

Author Manuscript Author Manuscript Author Manuscript Author Manuscript

and H). Neurite extension was observed to be proportional to the number of coils placed in the channels. Those with a low number of coils (TMM-L) showed a mixed population of round undifferentiated cells and some with neurites (Fig. 2G), whereas those in areas with a higher number of coils (TMM-H) exhibited longer neuron-like extensions (Fig. 2H). Neurite length was significantly longer in the TMM-H (87±14.6 mm) compared to the TMM-L area (55.76 ±12.53 mm; $p \leq 0.005$), and both were significantly higher compared to cells growing in control (CTR) channels (9.31±1.94 mm; $p \leq 0.001$). These observations indicate that the polymeric coils were able to release biologically active NGF into the luminal collagen matrix, forming a gradient at which low (TMM-L) and high (TMM-H) concentration areas can be established (Fig. 2I). This obsrvation was supported by quantification of protein release from the TMM-L and TMM-H regions of coils eluting BSA over 24 h, which confirmed a two-fold differential concentration at the TMM-H end (Fig. 1D). The amount of released NGF from both PLGA and PDO fibers was 44.0 and 53.6 pg/mm over 7 days, respectively, and approximately 4 mm in the low end and 8 mm of fiber in the high end. Therefore, the total amount of NGF released by the PLGA and PDO fibers in the microchannels was approximately 19.7 ng/ml/day and 24 ng/ml/day in the TMM-L region, respectively, and twice as much at the TMM-H end. The bioactivity of both fibers was determined by incubating them with PC12 cells and similar effects on neurite length were observed (Fig. 2E). To directly evaluate the concentration of biologically active NGF in the microchannel, PC12 cells were used as biosensors since they are known to respond linearly to a 10–100 ng/ml of NGF concentration by extending neurites that range from 5 to 120 μm in length (Gunning et al., 1981; Cao and Shoichet, 2001). We found the correlation between PC12 neurite length and NGF to be linear (Fig. 2J; R=0.86) and used the following equation to estimate the NGF concentration from the PC12 neurite length on the PLGA fiber coils.

$$[\mathrm{NGF}] = [(\text{PC12 neurite length} - 17.57)/(0.862)]$$

Using this formula it was determined that the neurite growth observed at TMM-L and TMM-H coiling regions of the TMM microchannels corresponded to 44 and 80 ng/ml of NGF, respectively (Fig. 2J). This result is in close agreement with the observed differences in protein release from these two regions and the concentration of NGF released by the polymeric fibers.

3.2. Modeling of protein microgradient diffusion

Next we designed a computer model to predict the NGF diffusion dynamics over time in the collagen filler of the TMM microchannels, and to compare the uniform and gradient coil configurations. The model calculated NGF concentrations in the collagen-filled microchannel (volume=0.49 μl) at the end of 1, 5 and 7 days are presented for both uniform and gradient coil configurations for comparison. For the uniform coil configuration, the release of NGF is expected to be consistent through the entire channel. The channel concentration reached a level of 7.5 ng/ml at day 1, and remain at ~7 ng/ml at day 7. As a result of proximal and distal diffusion, the uniformity in NGF distribution gradually increases while NGF concentration decreases. It results in a high concentration zone in the center of the channel; which may discourage neurons from continuing growth toward the

Author Manuscript Author Manuscript Author Manuscript Author Manuscript

distal end (Fig. 3A). In contrast, for gradient coil configuration, the release of NGF and resulting concentration distribution in the channel is non-uniform by design. Our results show the NGF concentration varies from 0.02 to 12.42 ng/ml at day 1. At day 7, the NGF concentration gradient is maintained with a minor decrease in the peak values to 9.53 ng/ml (Fig. 3A). The region of high NGF concentration corresponds to higher coil numbers. For the current set of design parameters, an average gradient of 0.02–10 ng/ml could be maintained over a week (Fig. 3B). Unlike the uniform coil, the gradient coil configuration provides sustained chemotactic gradients which continue to entice and to guide the growth of neurons toward the channel distal end. These results support the notion that a favorable, sustainable molecular gradient of biologically active growth factors can be established and maintained in the luminal collagen matrix by adjusting the number of coiled fibers on the walls of the agarose channels.

3.3. Nerve growth is enhanced and directed by 3D gradient growth factor delivery

The effect of different NGF concentrations on nerve regeneration was evaluated *in vitro* by measuring the number and length of axons that extended from neonatal DRGs placed at one end of the TMM gel (Fig. 4A). We compared control gels with no coils (Fig. 4B) to those with either 7 (Fig. 4C) or 14 coil turns (Fig. 4D). As expected, axonal growth was longer in the gels with NGF coils in comparison to the negative controls and increases significantly ($p \leq 0.005$; $n=4$) in the denser NGF coil group (1321±51.71 mm; 14 coil turns) compared to both the no growth factor (651.2±40.40 mm) and the low density coil groups (808.18±55.57 mm; 7 coil turns; Fig. 4F). The number of axons was also increased proportionally, however this trend was not statistically significant.

In a separate set of experiments we evaluated the effect of NGF gradient on DRG axonal extension. The growth of DRGs into microchannel coils with either uniform or gradient configurations in which the total NGF concentration was maintained by keeping the fiber length equal, showed enhanced axonal regeneration in the gradient preparation (Fig. 4E). Quantification of the axonal length confirmed a significant growth advantage ($p \leq 0.05$) of neurons growing through the collagen lumen and NGF gradient (1694±100.1 mm; $n=3$), compared to those containing a uniform growth factor concentration (1045±81.33 mm, $n=5$; Fig. 4G).

We also noted that neurite extension in the group with uniform distributed coils was often directed towards the coils on the walls of the microchannels, with axons following upward and downward trajectories seemingly following the helical direction of the coiled fibers, indicating an attraction to the expected NGF microgradients formed in between the coils (Fig. 5A). In sharp contrast, the neurites in the NGF gradient group showed robust linear growth in the middle of the microchannel, most axons in the G-NGF group seem to ignore the coils on the walls and follow a more linear path toward areas of higher NGF concentration (Fig. 5B). Quantification of the growth angle supported this notion as those in the U-NGF groups showed a broad directional growth ranging from +60° to −60°. Conversely, those presented in the G-NGF group showed a more directed growth, with angles ranging from +30° to −30° (Fig. 5C). Measurements of the turning angle ratio confirmed that the number of axons making sharper turns were significantly larger in the U-

Author Manuscript Author Manuscript Author Manuscript Author Manuscript

NGF compared to those in the G-NGF (0.54±0.06 n=4; 0.19±0.04 n=3, respectively; $p \leq 0.005$) respectively (Fig. 5D). Together, these data show that a robust chemotactic growth environment can be established three-dimensionally in multi-luminal scaffolds, by deploying a gradient of coiled polymeric fibers that release growth factors into the luminal collagen filler.

4. Discussion

This study reports on a method that establishes sustained three-dimensional NTF gradients in the collagen-filled lumen of multi-luminal nerve guides by placing biodegradable polymeric fibers on the wall of the microchannels. This method forms a stable chemotactic gradient within the luminal collagen, which is similar in composition to certain types of nerve multi-luminal nerve scaffolds (Tansey et al., 2011), and where the fiber coils can be tailored to the desired length, concentration gradient, and steepness. The benefit of NTF support for peripheral nerve regeneration has long been recognized and several reports have demonstrated the regenerative effects of NGF, FGF-1, GDNF and BDNF-supplemented nerve repair (Fine et al., 2002; Gordon et al., 2003; Allodi et al., 2012). However, the incorporation of luminal NTF gradients, known to guide adult injured neurons to their distal targets and needed for optimal nerve regeneration, remains a critical challenge (Uschold et al., 2007; Gordon, 2009). Current methods incorporate growth factors into the wall of hollow nerve guides (Tang et al., 2013), embed them directly into the gel matrix (Yang et al., 2005), or use microspheres or nanofibers placed directly into the lumen for NTF support (Madduri and Gander, 2012), all of which result in limited increments in axonal growth. Furthermore, these methods do not combine the NTFs gradients with ECM fillers such as fibronectin, collagen, or laminin (Bailey et al., 1993; Yu et al., 1999), and cannot provide multi-luminal gradients onto ECM-filled microchannels. This is particularly important as recent reports have shown that multi-luminal nerve scaffolds linearly guide nerve regeneration through lesion gaps, increase the surface growth area, and provide a regenerative advantage over simple hollow conduits (Tansey et al., 2011; Yao et al., 2010; Huang et al., 2010).

Here, we demonstrate that NGF-eluting polymeric coils can be used to establish three-dimensional concentration gradients in agarose microchannels and effectively induce neural differentiation of PC12 cells seeded in the collagen-filled lumen. Using computer modeling, we analyzed the diffusion dynamics of NGF from both uniform and gradient coils over 7 days. Results from gradient PLGA coils predict a luminal NGF concentration of 12.4 ng/ml, which is in agreement with our measured experimental release of 19.7 ng/ml/day from these polymeric coils. The model was also used to predict specific advantages of this method compared to gradients established from the walls of a hollow tube. The diffusion patterns from the NTF-coils through the complex material composition of multi-luminal nerve scaffolds (i.e., luminal collagen and agarose microchannels) formed unidirectional gradients that favor nerve regeneration, compared to that from NTF-eluting hollow tubes which are anticipated to form a central gradient, discouraging regeneration across the tube due to the rich environment inside the nerve guide.

Author Manuscript Author Manuscript Author Manuscript Author Manuscript

The notion of enhanced nerve regeneration by NGF gradients was confirmed experimentally through the significant increase in axonal length of DRG neurons exposed to a gradient compared to uniformly deployed coils at the same NGF concentration. Furthermore, the directionality of axonal growth within the collagen filled microchannels was positively affected by the presentation of the coils. In channels with uniform NGF-coil configuration, axons oriented their growth towards the individual coils making sharp turns from top to bottom along the microchannel, indicating the formation of microchemotactic gradients in between coils. In sharp contrast, those exposed to a NGF gradient ignored the coils and directed their growth towards the center of the microchannel lumen, consistent with the idea of linear chemotaxis along the microchannels. These data support the notion that gradient presentation of chemotactic molecules through the lumen is critical to achieve optimized linear nerve regeneration and improved repair.

The coil-based method reported here compares favorably to other proposed strategies for establishing highly controlled molecular gradients, as some are based on microfluidics and cannot be translated *in vivo* (Hjorto et al., 2009; Atencia et al., 2009; Motoo et al., 2008). Others rely on protein immobilization hindered by low protein loading efficacy (<4%) and minimal protein release (less than 0.05% in 8 days), and thus are inadequate for establishing chemotactic gradients of soluble proteins (Tang et al., 2013; Moore et al., 2006). It is also a viable alternative to methods that are effective in establishing chemotactic gradients for guided nerve regeneration *in vivo*, but which depend on differential injections of replication-defective viral vectors, which are difficult to implement in the clinic (Hu et al., 2010; Zochodne, 2012). Furthermore, the amount of NGF in the channels needed to achieve a robust nerve regeneration effect (0.5–10 ng/ml per day) is substantially smaller compared to the higher doses reported by others (i.e., 0.5–20 μg/day) and thus less likely to produce deleterious effects due to NTF overdose (Boyd and Gordon, 2002).

The present method is also highly flexible, allowing the independent loading of growth factors in different microchannels of the same multi-luminal device (Fig. 6A), such that the content of the trophic support can be tailored to individual nerves with different sensory submodality or motor fiber content. For instance, mixed nerves can be repaired with multi-luminal nerve scaffolds with different NTF in separate channels to favor the differential regeneration of sensory and motor type fascicles. In one form, NGF can be used to enrich C-fiber axons that selectively express the TrkA receptors (Zochodne, 2012; Hu et al., 2010), while NT-3 can be used to entice the regeneration of proprioceptive axons that uniquely express the TrkC receptor (Chen et al., 2002). This strategy has been recently demonstrated as a feasible mechanism to molecularly control the modality composition of the regenerated nerves (Hu et al., 2010; Zochodne, 2012; Grill et al., 1997; Lotfi et al., 2011). The present method takes this notion a step further, in that it allows the possibility of defining the modality composition of the regenerated nerve at a fascicular level with high molecular control.

This method also allows for the fabrication of devices with bilateral gradients, which are particularly pertinent for the repair of the injured spinal cord (Fig. 6B), where transection injuries affect a mixed population of descending motor axons that innervate the ventral motor neuron pool, and ascending sensory axons that innervate relay centers in the anterior

Author Manuscript Author Manuscript Author Manuscript Author Manuscript

spinal cord, brain stem and thalamus. Several studies have reported the benefit of using growth factors to mediate nerve regeneration across the injury site in the adult spinal cord. Indeed, BDNF, NT-3 and NT4–5 have all been reported to induce the regeneration of several neuron types (Grill et al., 1997; Blesch et al., 2004; Brock et al., 2010). In addition, GDNF seems to preferentially entice descending proprioceptive axons (Deng et al., 2013), while NGF seems to favor separate groups of motor and sensory ascending sensory afferents (Grill et al., 1997). Thus, the ability to provide opposite directional gradients with growth factors tailored for specific descending and ascending axons in separate microchannels may prove beneficial in the biomimetic design of tissue engineered scaffolds for improved fiber tract repair in the injured spinal cord.

5. Conclusions

We report a simple and reproducible method based on the anchoring of protein loaded polymeric coils onto the wall of multi-luminal hydrogel nerve conduits to provide multi-luminal growth factor gradient support for neural gap repair. This method is highly tunable and allows for the enhancement and direction of nerve regeneration through the establishment of chemotaxis in collagen-filled multi-luminal devices, thus optimizing linear nerve regeneration and potentially improving tissue repair strategies.

Acknowledgments

We thank Dr. Jennifer Seifert for suggestions on the preparation of the manuscript, Eduardo Martinez, and Dr. Swarup Dash for collaborative assistance. We also thank Drs. Kevin Nelson and Brent Crow for the manufacturing of the polymeric fiber coils. This work was supported by a NIH/NINDS R21NS072955-01A1 Grant (MIR).

References

Adams DN, Kao EYC, Hypolite CL, Distefano MD, Hu WS, Letourneau PC, 2005. Growth cones turn and migrate up an immobilized gradient of the laminin IKVAV peptide. J. Neurobiol 62, 134–147. [PubMed: 15452851]

Allodi I, Udina E, Navarro X, 2012. Specificity of peripheral nerve regeneration: interactions at the axon level. Prog. Neurobiol 98, 16–37. [PubMed: 22609046]

Arimura N, Kaibuchi K, 2007. Neuronal polarity: from extracellular signals to intracellular mechanisms. Nat. Rev. Neurosci 8, 194–205. [PubMed: 17311006]

Atencia J, Morrow J, Locascio LE, 2009. The microfluidic palette: a diffusive gradient generator with spatio-temporal control. Lab Chip 9, 2707–2714. [PubMed: 19704987]

Bailey SB, Eichler ME, Villadiego A, Rich KM, 1993. The influence of fibronectin and laminin during Schwann cell migration and peripheral nerve regeneration through silicon chambers. J. Neurocytol 22, 176–184. [PubMed: 8478639]

Blesch A, Yang H, Weidner N, Hoang A, Otero D, 2004. Axonal responses to cellularly delivered NT-4/5 after spinal cord injury. Mol. Cell. Neurosci 27, 190–201. [PubMed: 15485774]

Boyd JG, Gordon T, 2002. A dose-dependent facilitation and inhibition of peripheral nerve regeneration by brain-derived neurotrophic factor. Eur. J. Neurosci 15, 613–626. [PubMed: 11886442]

Brock JH, Rosenzweig ES, Blesch A, Moseanko R, Havton LA, Edgerton VR, et al., 2010. Local and remote growth factor effects after primate spinal cord injury. J. Neurosci 30, 9728–9737. [PubMed: 20660255]

Cao X, Shoichet MS, 2001. Defining the concentration gradient of nerve growth factor for guided neurite outgrowth. Neuroscience 103, 831–840. [PubMed: 11274797]

Author Manuscript Author Manuscript Author Manuscript Author Manuscript

Chen HH, Tourtellotte WG, Frank E, 2002. Muscle spindle-derived neurotrophin 3 regulates synaptic connectivity between muscle sensory and motor neurons. J. Neurosci 22, 3512–3519. [PubMed: 11978828]

Dawood A, Lotfi P, Dash S, Kona S, Nguyen K, Romero-Ortega M, 2011. VEGF release in multiluminal hydrogels directs angiogenesis from adult vasculature. Cardiovasc. Eng. Technol 2, 173–185.

Deng LX, Deng P, Ruan Y, Xu ZC, Liu NK, Wen X, et al., 2013. A novel growth-promoting pathway formed by GDNF-overexpressing Schwann cells promotes propriospinal axonal regeneration, synapse formation, and partial recovery of function after spinal cord injury. J. Neurosci 33, 5655–5667. [PubMed: 23536080]

Dickson BJ, 2002. Molecular mechanisms of axon guidance. Science 298 (5600), 1959–1964. [PubMed: 12471249]

Dodla MC, Bellamkonda RV, 2008. Differences between the effect of anisotropic and isotropic laminin and nerve growth factor presenting scaffolds on nerve regeneration across long peripheral nerve gaps. Biomaterials 29, 33–46. [PubMed: 17931702]

Fine EG, Decosterd I, Papaloizos M, Zurn AD, Aebischer P, 2002. GDNF and NGF released by synthetic guidance channels support sciatic nerve regeneration across a long gap. Eur. J. Neurosci 15, 589–601. [PubMed: 11886440]

Flanagan JG, 2006. Neural map specification by gradients. Curr. Opin. Neurobiol 16, 59–66. [PubMed: 16417998]

Gallo G, Letourneau PC, 1999. Axon guidance: a balance of signals sets axons on the right track. Curr. Biol 9, R490–R492. [PubMed: 10395535]

Gordon T, 2009. The role of neurotrophic factors in nerve regeneration. Neurosurg. Focus 26, E3.

Gordon T, Sulaiman O, Boyd JG, 2003. Experimental strategies to promote functional recovery after peripheral nerve injuries. J. Peripher. Nerv. Syst 8, 236–250. [PubMed: 14641648]

Grill R, Murai K, Blesch A, Gage FH, Tuszynski MH, 1997. Cellular delivery of neurotrophin-3 promotes corticospinal axonal growth and partial functional recovery after spinal cord injury. J. Neurosci 17, 5560–5572. [PubMed: 9204937]

Grill RJ, Blesch A, Tuszynski MH, 1997. Robust growth of chronically injured spinal cord axons induced by grafts of genetically modified NGF-secreting cells. Exp. Neurol 148, 444–452. [PubMed: 9417824]

Gunning PW, Landreth GE, Layer P, Ignatius M, Shooter EM, 1981. Nerve growth factor-induced differentiation of PC12 cells: evaluation of changes in RNA and DNA metabolism. J. Neurosci 1, 368–379. [PubMed: 7264725]

Hjorto GM, Hansen M, Larsen NB, Kledal TN, 2009. Generating substrate bound functional chemokine gradients in vitro. Biomaterials 30, 5305–5311. [PubMed: 19577290]

Hu X, Cai J, Yang J, Smith GM, 2010. Sensory axon targeting is increased by NGF gene therapy within the lesioned adult femoral nerve. Exp. Neurol 223, 153–165. [PubMed: 19733564]

Huang J, Lu L, Hu X, Ye Z, Peng Y, Yan X, et al., 2010. Electrical stimulation accelerates motor functional recovery in the rat model of 15-mm sciatic nerve gap bridged by scaffolds with longitudinally oriented microchannels. Neurorehabil. Neural Repair 24, 736–745. [PubMed: 20702391]

Kapur TA, Shoichet MS, 2004. Immobilized concentration gradients of nerve growth factor guide neurite outgrowth. J. Biomed. Mater. Res. A 68, 235–243. [PubMed: 14704965]

Kolodkin AL, Tessier-Lavigne M, 2011. Mechanisms and molecules of neuronal wiring: a primer. Cold Spring Harb. Perspect. Biol 3, 1–14.

Lotfi P, Garde K, Chouhan AK, Bengali E, Romero-Ortega MI, 2011. Modality-specific axonal regeneration: toward selective regenerative neural interfaces. Front. Neuroeng 4, 1–11. [PubMed: 21270946]

Madduri S, Gander B, 2012. Growth factor delivery systems and repair strategies for damaged peripheral nerves. J. Controlled Release: Off. J. Controlled Release Soc 161, 274–282.

Moore K, MacSween M, Shoichet M, 2006. Immobilized concentration gradients of neurotrophic factors guide neurite outgrowth of primary neurons in macroporous scaffolds. Tissue Eng. 12, 267–278. [PubMed: 16548685]

Author Manuscript Author Manuscript Author Manuscript Author Manuscript

Motoo K, Toda N, Arai F, Fukuda T, Sekiyama K, Nakajima M, 2008. Generation of concentration gradient from a wave-like pattern by high frequency vibration of liquid–liquid interface. Biomed. Microdevices 10, 329–335. [PubMed: 18071908]

Murray JD, 1989. Reaction Diffusion, Chemotaxis and Non-local Mechanisms. Mathematical Biology. Springer 232–253.

Nelson KD, Romero A, Waggoner P, Crow B, Borneman A, Smith GM, 2003. Technique paper for wet-spinning poly (L-lactic acid) and poly(DL-lactide-co-glycolide) monofilament fibers. Tissue Eng. 9, 1323–1330. [PubMed: 14670119]

Ramanujan S, Pluen A, McKee TD, Brown EB, Boucher Y, Jain RK, 2002. Diffusion and convection in collagen gels: implications for transport in the tumor interstitium. Biophys. J 83, 1650–1660. [PubMed: 12202388]

Romero MI, Rangappa N, Garry MG, Smith GM, 2001. Functional regeneration of chronically injured sensory afferents into adult spinal cord after neurotrophin gene therapy. J. Neurosci 21, 8408–8416. [PubMed: 11606629]

Song H, Poo M, 2001. The cell biology of neuronal navigation. Nat. Cell Biol 3, E81–E88. [PubMed: 11231595]

Tang S, Zhu J, Xu Y, Xiang AP, Jiang MH, Quan D, 2013. The effects of gradients of nerve growth factor immobilized PCLA scaffolds on neurite outgrowth in vitro and peripheral nerve regeneration in rats. Biomaterials 34, 7086–7096. [PubMed: 23791502]

Tang XQ, Heron P, Mashburn C, Smith GM, 2007. Targeting sensory axon regeneration in adult spinal cord. J. Neurosci 27, 6068–6078. [PubMed: 17537979]

Tansey K, Seifert J, Botterman B, Delgado M, Romero M, 2011. Peripheral nerve repair through multi-luminal biosynthetic implants. Ann. Biomed. Eng 39, 1815–1828. [PubMed: 21347549]

Tonra JR, Curtis R, Wong V, Cliffer KD, Park JS, Timmes A, et al., 1998. Axotomy upregulates the anterograde transport and expression of brain-derived neurotrophic factor by sensory neurons. J. Neurosci 18, 4374–4383. [PubMed: 9592114]

Uschold T, Robinson GA, Madison RD, 2007. Motor neuron regeneration accuracy: balancing trophic influences between pathways and end-organs. Exp. Neurol 205, 250–256. [PubMed: 17368445]

Wu J, Mao Z, Tan H, Han L, Ren T, Gao C, 2012. Gradient biomaterials and their influences on cell migration. Interface Focus 2, 337–355. [PubMed: 23741610]

Yang Y, De Laporte L, Rives CB, Jang JH, Lin WC, Shull KR, et al., 2005. Neurotrophin releasing single and multiple lumen nerve conduits. J. Controlled Release: Off. J. Controlled Release Soc 104, 433–446.

Yao L, de Ruiter GC, Wang H, Knight AM, Spinner RJ, Yaszemski MJ, et al., 2010. Controlling dispersion of axonal regeneration using a multichannel collagen nerve conduit. Biomaterials 31, 5789–5797. [PubMed: 20430432]

Yu X, Dillon GP, Bellamkonda RB, 1999. A laminin and nerve growth factor-laden three-dimensional scaffold for enhanced neurite extension. Tissue Eng. 5, 291–304. [PubMed: 10477852]

Ziemba KS, Chaudhry N, Rabchevsky AG, Jin Y, Smith GM, 2008. Targeting axon growth from neuronal transplants along preformed guidance pathways in the adult CNS. J. Neurosci 28, 340–348. [PubMed: 18184776]

Zilberman M, 2005. Dexamethasone loaded bioresorbable films used in medical support devices: structure, degradation, crystallinity and drug release. Acta Biomater. 1, 615–624. [PubMed: 16701842]

Zochodne DW, 2012. The challenges and beauty of peripheral nerve regrowth. J. Peripher. Nerv. Syst 17, 1–18.

Author Manuscript
Author Manuscript
Author Manuscript
Author Manuscript

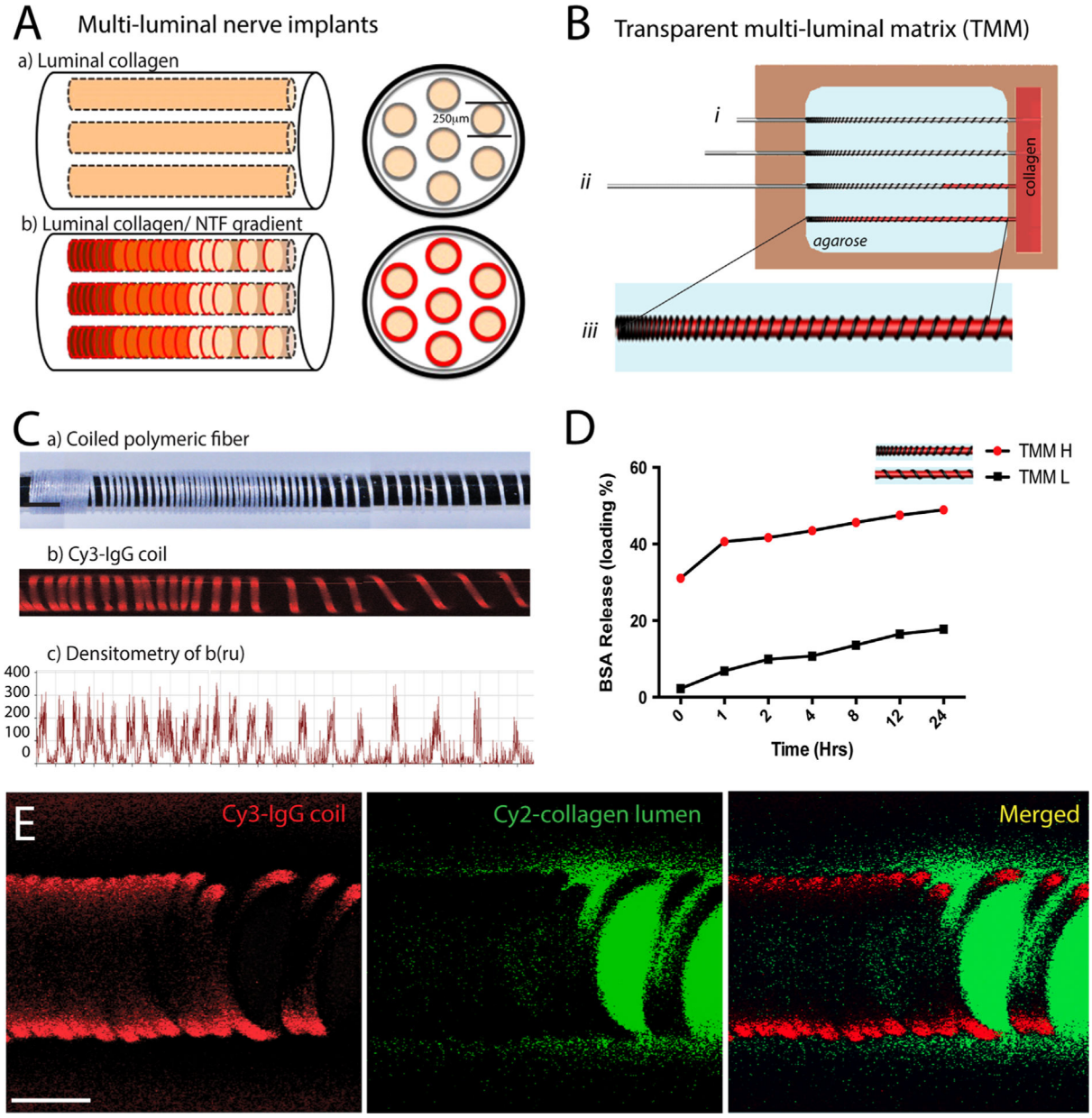

Fig. 1 –.

Coiled polymeric fibers form molecular gradients in collagen-filled hydrogel microchannels: (A) schematic of current multi-luminal nerve implant designs compared to one with luminal NTF release by coiled polymeric fibers in the microchannels. (B) Illustration of the TMM casting device. Removal of the metal rods after agarose gelation anchors the polymer coils onto the walls of the microchannels while simultaneously filling the lumen with collagen (i)–(iii). (C) Fluorescence imaging and densitometry demonstrate the gradient formed Cy3-PLGA fiber coil. (D) BSA PLGA fiber coils release high (H) and low (L) concentration according to the number of coils. (E) Confocal micrograph showing the deployed polymeric Cy3-coil (red) in the agarose gel (i.e., black since agarose is transparent) with Cy2-labled collagen in the lumen (green). Scale bar=100 μm.

Author Manuscript Author Manuscript Author Manuscript Author Manuscript

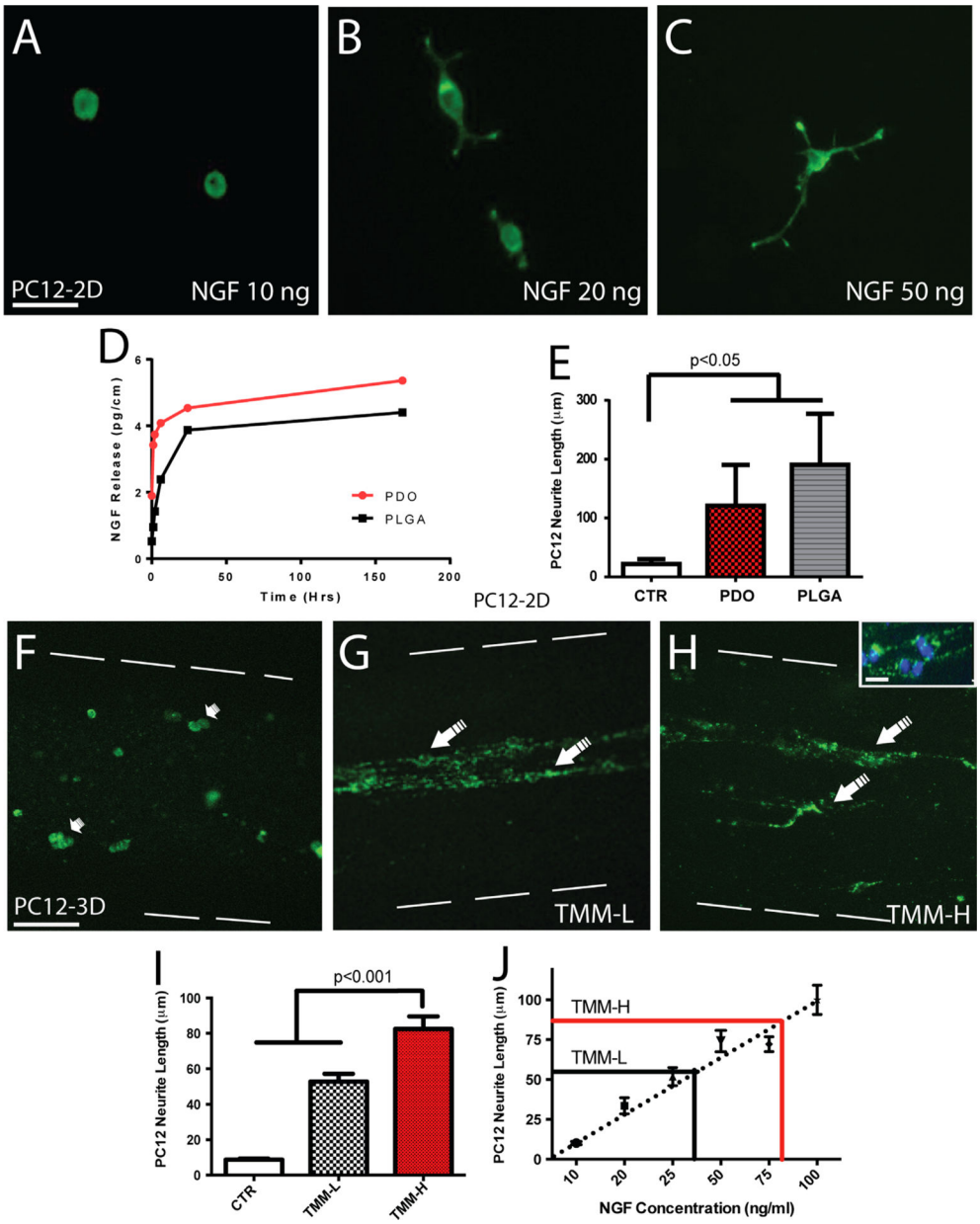

Fig. 2 –.

PC12 cell differentiation in a three-dimensional NGF gradient. PC12 cells differentiate in the presence of NGF elongating their neurites in direct proportion to NGF concentration: (A) 10 ng/ml, (B) 20 ng/ml, (C) 50 ng/ml, (D) NGF release profiles from PLGA and PDO fibers, and (E) comparable PC12 cell differentiated induced by PLGA and PDO fibers, both of which are significantly different compared to BSA controls. Images of PC12 cells cultured in the TMM collagen-filled agarose microchannels in which empty coils (F), low NGF (G) or high NGF (H) coils were deployed. Flattened 3D confocal images showed undifferentiated PC12 cells in the control group (small arrows in (F)). In contrast, cells with extended neurites were seen in those with NGF-releasing coils (large arrows in (G) and (H)). The inset shows a higher magnification of the PC12 cells in the microchannels with DAPI-

Author Manuscript Author Manuscript Author Manuscript Author Manuscript

stained nuclei. Neurite length increased significantly in both the TMM-L and TMM-H NGF coils compared to controls (I). (J) Calibration curve of neurite length of PC12 cells shows the estimated release of biologically active NGF as reported by these cells in the microchannels. Scale bar=50 μm (A), 100 μm (F), and 10 μm (H inset).

Author Manuscript Author Manuscript Author Manuscript Author Manuscript

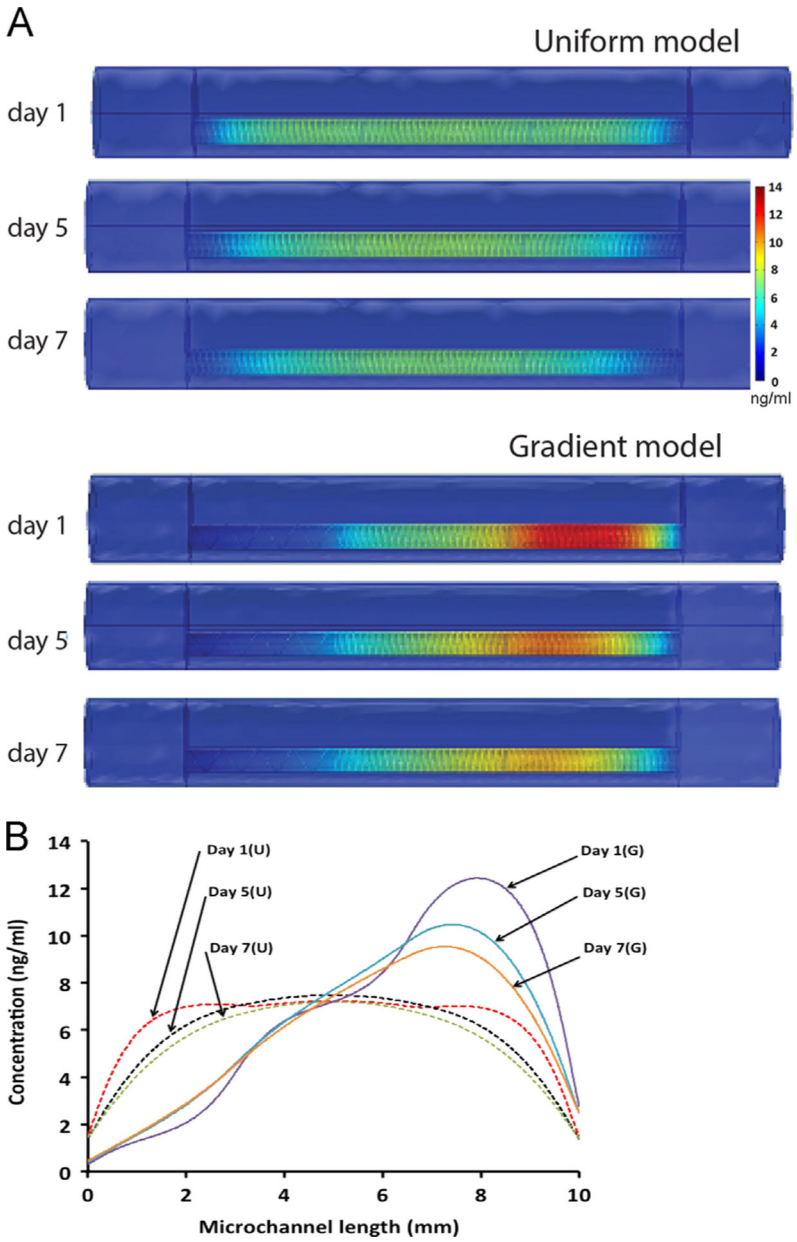

Fig. 3 –.

Finite element simulation of NGF diffusion from polymer coiled fibers: (A) the uniform distribution of the coils results in even diffusion of NGF across the microchannel over 1–7 days with some dilution at the openings. The differential deployment of coiled fibers results in a 1–12 ng/ml NGF concentration gradient with a steep angle of 22°, which increases and expands overtime to cover most of the volume of the microchannel. (B) This difference is accentuated when the uniform and gradient concentrations are compared along the longitudinal axis.

Author Manuscript
Author Manuscript
Author Manuscript
Author Manuscript

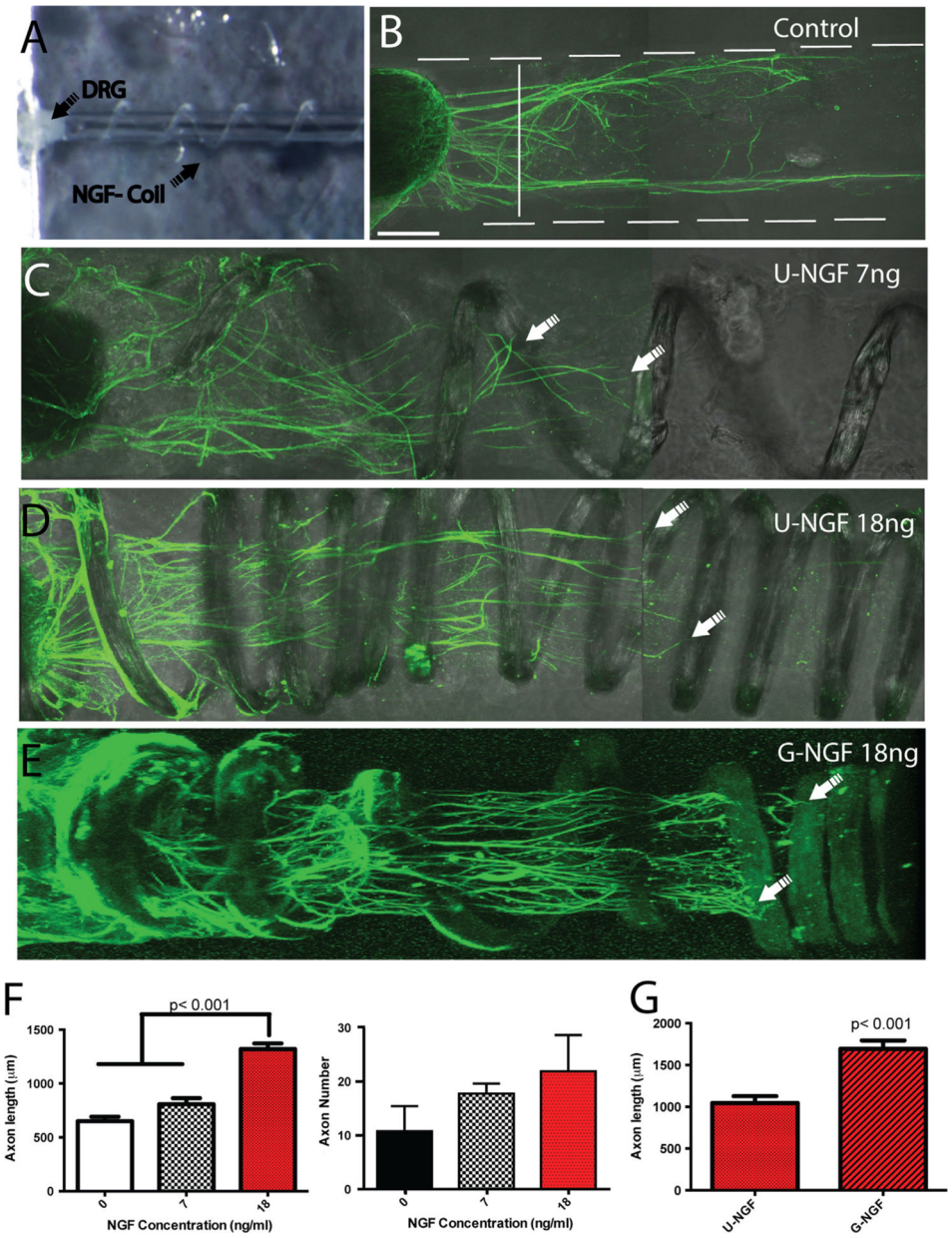

Fig. 4 –.

Coiled NGF-eluting fibers entice DRG axonal growth: (A) DIC images of the TMM gel showing a microchannel and a DRG explant at the proximal end. The microchannel is filled with air for better visualization. Flattened 3D confocal images of the DRG axonal growth immunolabeled for β-tubulin visualization (green) is shown for TMM gels with: (B) no coils, (C) coils with uniform 7 ng of NGF, and (D) coils with 18 ng of NGF. (E) Gradient configuration. (F) Axon length increased significantly at the higher NGF concentration, while a non-significant trend was observed in increased axonal number on the NGF-eluting groups. (G) The gradient presentation showed a significant increase in the axonal length of neurons growing towards an increasing NGF concentration (n=3–5). Scale bar=100 μm (B)–(E).

Author Manuscript Author Manuscript Author Manuscript Author Manuscript

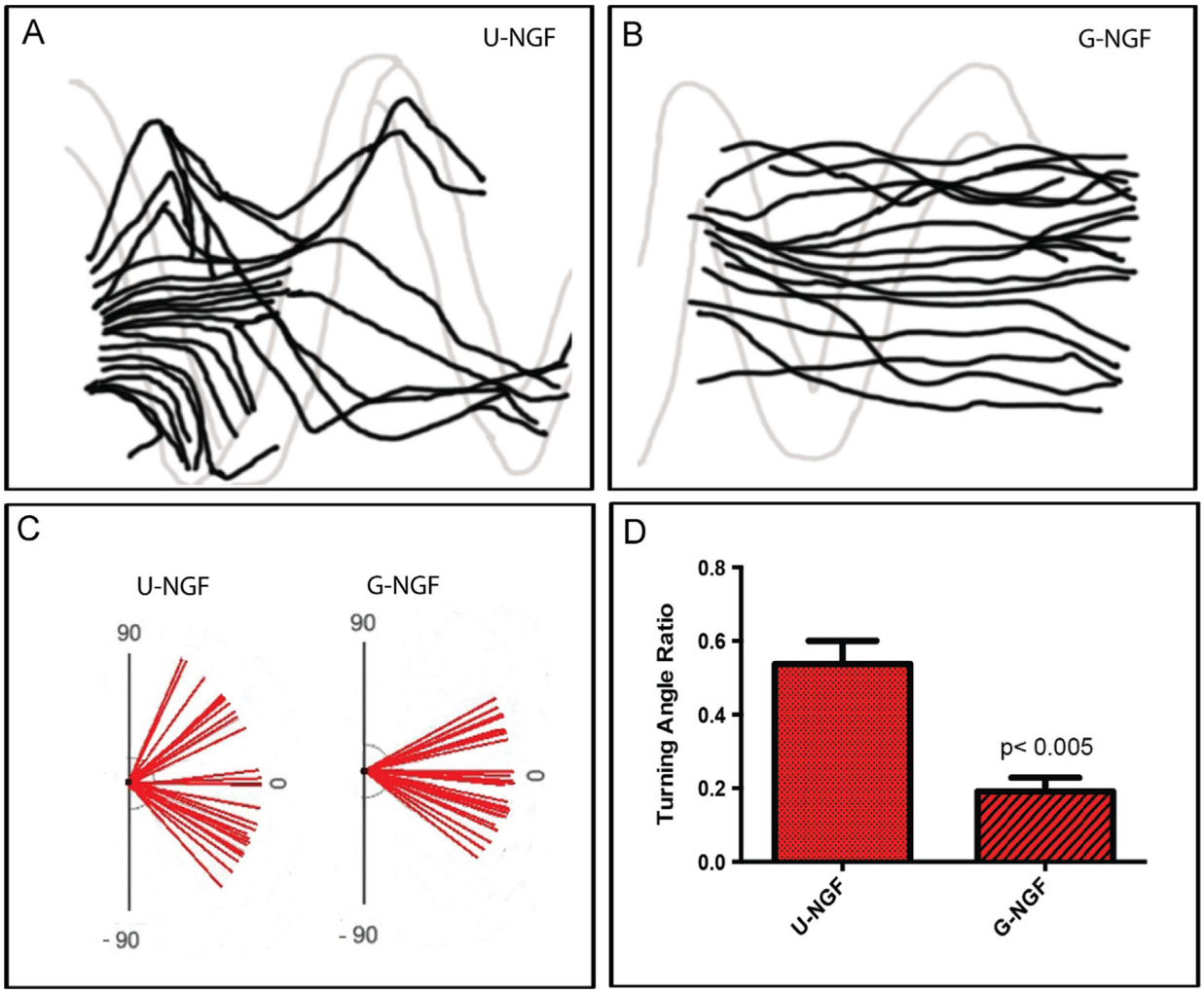

Fig. 5 –.

Chemotactic effect of NGF gradients. Camera lucida tracings of axons in uniform (A) or gradient NGF (B) microchannels. (C) Direction of axonal growth and (D) turning angles show more linearly directed axonal growth within G compared to U microchannels.

Author Manuscript Author Manuscript Author Manuscript Author Manuscript

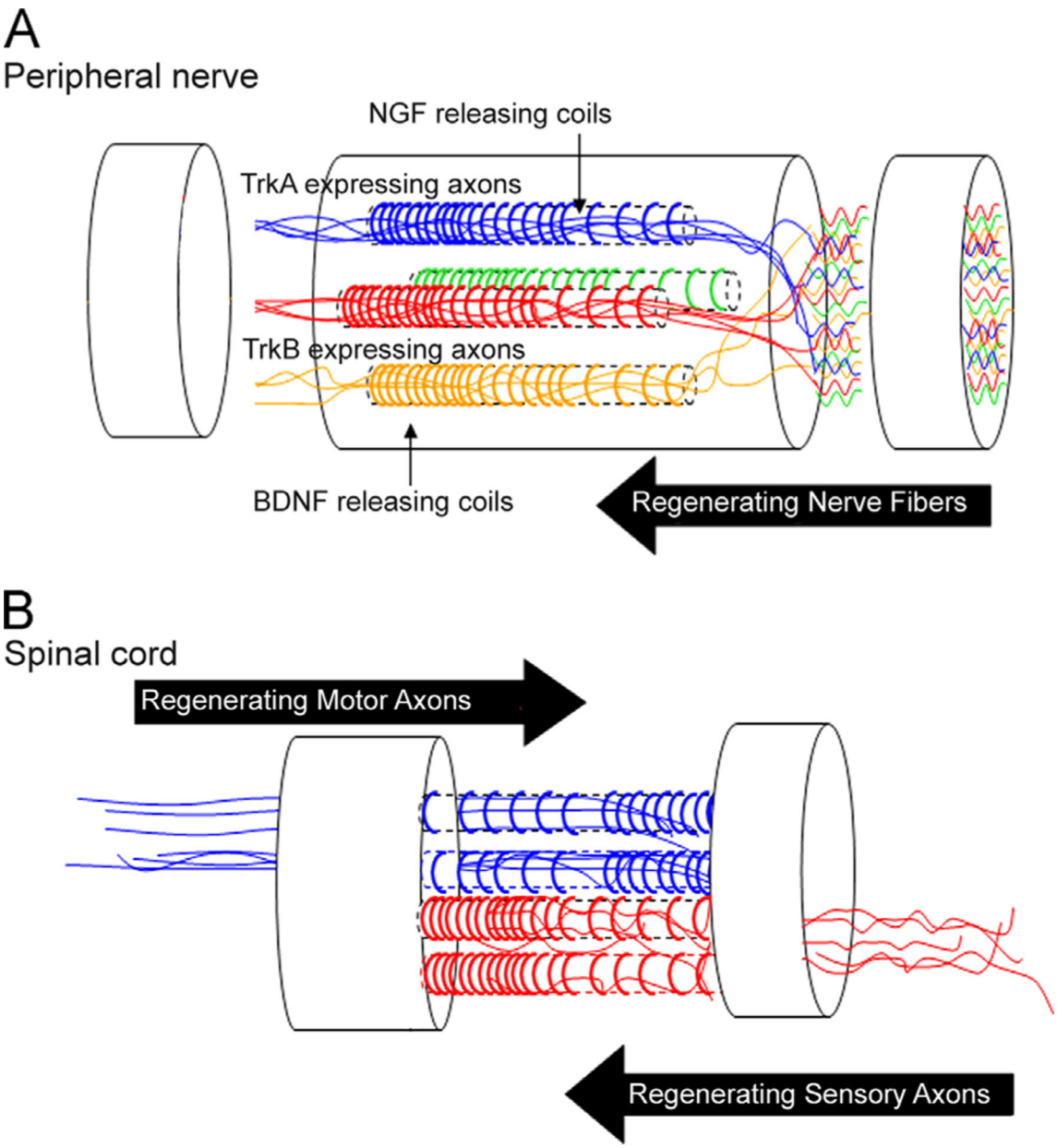

Fig. 6 –.

Schematic diagram representing G-coiled fibers with different NTFs targeted for specific modality axons: (A) the polymeric coils illustrated in different colors in separate channels represent distinct growth factor gradients (i.e., NGF, NT-3, BDNF) that can be designed to entice the axonal growth of a defined population of specific neurons. (B) The method can be tailored to fabricate bilateral gradients, which are particularly important for the repair of the injured spinal cord.

Author Manuscript Author Manuscript Author Manuscript Author Manuscript

Table 1 –

Diffusivities and dimensions used for the device and the FE model.

Parameter	Value	Description
$D_{collagen}$	7.6×10^{-12} m^2/s (Ramanujan et al., 2002; Tansey et al., 2011)	Diffusivity of drug molecules in 0.1% collagen
$D_{agarose}$	$2.31 \times 10^{-14} m^2/s$ (Ramanujan et al., 2002; Tansey et al., 2011)	Diffusivity of drug molecules in 1.5% agarose
OD, ID	3 mm & 1.5 mm	Outer & Inner diameter of external tubing
L	10 mm	Length of the device and the microchannel
$d_{microchannel}$	250 μm	Diameter of collagen-filled microchannel
d_{coil}	50 μm	Diameter of PLGA drug releasing coil